Dual-Mode Bridge-Shaped Dielectric Resonator Antennas

Georgios Almpanis, Christophe Fumeaux, *Senior Member, IEEE*, and Rüdiger Vahldieck, *Fellow, IEEE*

***Abstract*—Different configurations of bridge-shaped dielectric resonator antennas (b-DRAs) made of high-permittivity materials are presented in this letter. These DRA geometries can be seen as an evolution of the notched rectangular DRAs introduced by other authors, but their operational principle is different. The particularities and advantages of the proposed geometry will be investigated and demonstrated for a single bridge first. Afterward, the concept will be extended to two realizations of well-operating dual-mode b-DRAs with stable radiation patterns and low cross polarization. For the analysis of these structures, a full-wave analysis solver (HFSS) was used. Prototype fabrication and measurements confirm the results of the simulations.**

***Index Terms*—Aperture coupling, dielectric resonator antennas (DRAs), dual-mode operation.**

I. Introduction

BEFORE the introduction of dielectric resonator antennas (DRAs) by Long *et al.* [1] in 1983, dielectric resonators (DRs) were primarily used for filter applications in microwave circuits. They were made out of low-loss high-permittivity materials and operated in their higher order modes. The observation, however, that the lower order modes of open DRs exhibit low Q-factors, and therefore high "radiation losses," led to the first dielectric structures being used as radiating elements. Since then, DRAs have received increasing attention due to their inherent attributes of high radiation efficiency, compact size, and high versatility in terms of their shape, their feeding mechanisms, and their excited modes.

Another very important feature of the DRAs, which is decisively affecting their character and their radiation properties, is their inherent ability to effectively fill the radian sphere [2]. Volumetric sources like DRAs radiate throughout their entire volume, and therefore the amount of energy radiated from such radiators is considerably larger than the energy stored in their near fields. Thus, the radiation Q-factor of the DRAs is smaller and their impedance bandwidth is larger than that of the typical resonant antennas.

Manuscript received September 25, 2009; manuscript revised November 11, 2009. Date of publication January 22, 2010; date of current version March 16, 2010. This work was supported by ETH Research Grant TH-38/04-1.

G. Almpanis and R. Vahldieck are with the Laboratory for Electromagnetic Fields and Microwave Electronics, ETH Zurich, 8092 Zurich, Switzerland (e-mail: almpanis@ifh.ee.ethz.ch).

C. Fumeaux is with the School of Electrical and Electronic Engineering, The University of Adelaide, Adelaide, SA 5005, Australia (e-mail: cfumeaux@eleceng.adelaide.edu.au).

Color versions of one or more of the figures in this letter are available online at http://ieeexplore.ieee.org.

Digital Object Identifier 10.1109/LAWP.2010.2041177

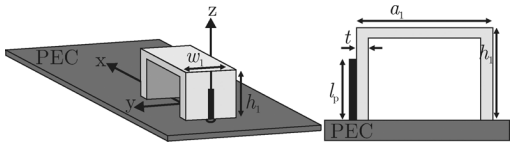

Fig. 1. General and side view of the basic probe-fed bridge-shaped DRA.

As the operation mechanism of the DRAs is connected with their volumetric nature, it is clear that the geometry and the electrical properties of the dielectric resonators are crucial factors for the determination and the improvement of their radiation characteristics. The strong relation between the dielectric resonator geometry (shape and materials) and its operational properties has been extensively demonstrated in the literature [3]–[8]. For example, an inversed trapezoidal DRA and an inversed pyramidal DRA were presented in [3] and [4], respectively, demonstrating a wide impedance bandwidth and well-behaved broadside radiation patterns. An annular DRA exhibiting a 3:1 impedance bandwidth and monopole-like radiation patterns was investigated in [5]. Furthermore, various multilayer DRAs in rectangular [6] and cylindrical [7] configurations have demonstrated that the combination of different materials can be exploited to enhance the bandwidth of DRA operation. Finally, a notched rectangular DRA demonstrating a 28% wide bandwidth and broadside patterns was investigated in [8]. This DRA comprised an aperture-fed rectangular parallelepiped whose central part had been removed. The empty space within the dielectric resonator volume results in a smaller confinement of the fields inside the dielectric and, therefore, in a wider DRA bandwidth. In this particular DRA, the relative permittivity of the dielectric resonator is chosen to have a relatively small value ($\varepsilon_r = 10.8$), with the consequence that the size of the notch has to be kept quite small to achieve sufficient coupling between the feed and the dielectric resonator [9]. As a result, it is difficult to use the empty region within the DRA for other purposes.

Based on the above observations on the advantages and the limitations of the notched DRAs, the present letter introduces an evolution toward a versatile DRA geometry that can be used as a building element for various advanced DRA structures. This structure is called bridge-shaped DRA (b-DRA) and is illustrated in Fig. 1. The b-DRA shape appears similar to that of the notched rectangular DRA of [8]. However, two crucial differences can be identified: First the b-DRA is constructed from a high-dielectric-permittivity material, and second, it uses only thin material plates, resulting in notch dimensions larger than

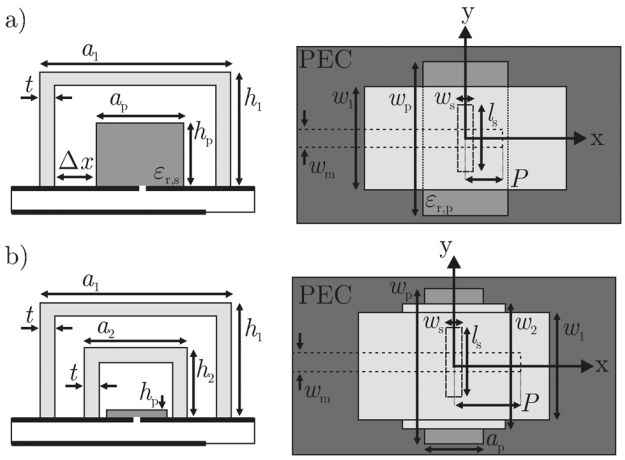

Fig. 2. Side and top views of dual-mode aperture-fed b-DRA configurations: (a) b-DRA coupled with a rectangular DRA; (b) double b-DRA.

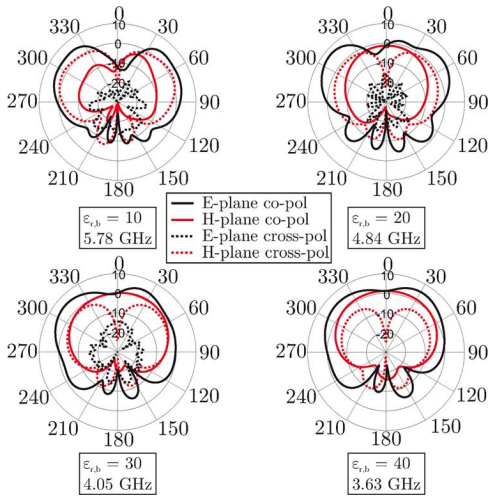

Fig. 3. Simulated radiation patterns (at the resonance frequency) of the b-DRA for identical geometry but different values of its dielectric permittivity $\varepsilon_{\mathrm{r,b}} = 10, 20, 30,$ and 40. The graphs illustrate the transition from a loaded-monopole radiation pattern to the broadside pattern of a magnetic-monopole, which corresponds to the fundamental TE_{111} mode of a rectangular DRA.

for the notched DRA. Because of that, the b-DRA can be interpreted as a dielectric half-loop, and its operation and geometrical features present advantages that could make it a potential candidate for various applications.

The application of DRAs as a packaging cover has been demonstrated in [10]. The present bridge implementation provides an extension of the concept that can help overcome several antenna-packaging-related problems. As an example, some of the components in a RF front end can be placed in the empty space within the bridge volume so that they are protected from various mechanical and/or climatic conditions. In addition to that, the dielectric bridge may incorporate other radiating elements, sharing the same volume, in order to improve the antenna's bandwidth response or to obtain a multimode operation with well-defined broadside radiation patterns. Two representative examples of aperture-fed dual-mode b-DRAs are shown in Fig. 2. These examples will be examined in the following sections of this letter.

II. Probe-Fed b-DRA

A test configuration of a probe-fed b-DRA is illustrated in Fig. 1. The coaxial probe is first selected as the feeding scheme of the b-DRA because of its operational and design simplicity. In the following numerical analysis, the bridge-shaped dielectric resonator with dielectric permittivity $\varepsilon_{\mathrm{r}} = 40$ takes the arbitrarily selected dimensions $a_1 = 20$ mm, $w_1 = 12$ mm, $h_1 = 16$ mm, and $t = 1$ mm. The b-DRA is mounted on a ground plane of dimensions 120×100 mm^2, and it is coupled through a coaxial probe of length $l_{\mathrm{p}} = 9.4$ mm optimized for best matching.

Provided that the b-DRA is excited in its lowest-order mode, its radiation characteristics are comparable to those of the TE_{111} mode of the rectangular DRA. In other words, a b-DRA and a canonical rectangular DRA can be regarded as equivalent radiating structures. The "effective" permittivity of the rectangular DRA equivalent to a given b-DRA is then a function of the bridge dielectric permittivity and of the relative volumes of the dielectric resonator and air under the bridge. An approximate value for this effective permittivity can be found as the volume-fraction weighted average of the permittivities involved. To demonstrate the equivalence between the b-DRA and the rectangular DRA, let us assume that the permittivity of the b-DRA is ranging from $\varepsilon_{\mathrm{r,b}} = 10$ to $\varepsilon_{\mathrm{r,b}} = 40$. Simulations are performed using Ansoft HFSS. For selected bridge permittivity values, the radiation patterns and the resonance frequency of the lowest-order mode of the b-DRA are provided in Fig. 3. It can be observed in the figure that for low values of the dielectric permittivity ($\varepsilon_{\mathrm{r,b}} = 10$), the radiation patterns of the DRA structure are monopole-like. It is thus clear that in this case the probe is the radiating element and the dielectric bridge has just the role of a dielectric loading. This can be intuitively understood if we consider the equivalent rectangular DRA. Since the permittivity of the bridge-shaped resonator is low and the volume of the dielectric bridge is small compared to that of the notch, the effective permittivity of the rectangular DRA is very low, i.e., well under 10. As a result, the coupling between the feed and the dielectric resonator becomes very weak, and subsequently the radiation from the feeding probe becomes dominant. As the permittivity $\varepsilon_{\mathrm{r,b}}$ increases, the b-DRA resonance frequency drops and, at the same time, the coupling to the dielectric resonator becomes stronger. Hence, the TE_{111} mode is more efficiently excited and consequently the radiation patterns become broadside. This trend is clearly observed in Fig. 3 for the cases $\varepsilon_{\mathrm{r,b}} = 30$ and 40. It is now clear that a bridge-shaped dielectric resonator of a relatively high dielectric permittivity can exhibit similar radiation properties as a canonical rectangular DRA of a much lower permittivity. In addition to that, the operational bandwidth of the b-DRA is also similar to that of the rectangular DRA since the notch within the b-DRA volume makes up for the high permittivity value of the resonator. In terms of design, starting dimensions for simulation and optimization of the b-DRA can be found by using the design formulas for a rectangular DRA [9] and an effective permittivity approximated as the volume-fraction weighted average of the permittivity of the bridge and air.

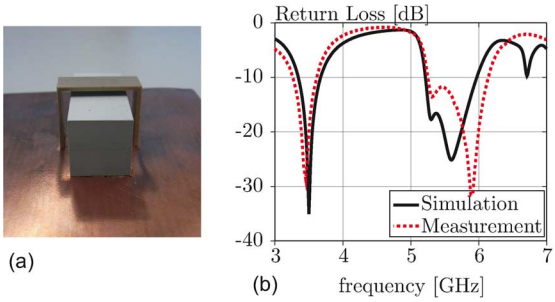

Fig. 4. (a) Fabricated prototype of the aperture-fed b-DRA coupled to a rectangular DRA. (b) Simulated and measured return loss.

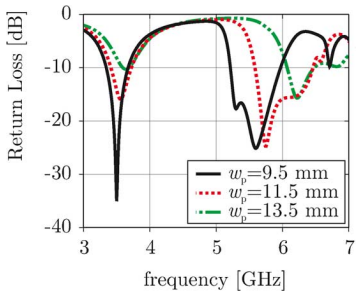

Fig. 5. Simulated return loss of the dual-mode aperture-fed b-DRA for different values of the slab dimension $w_{\rm p}$.

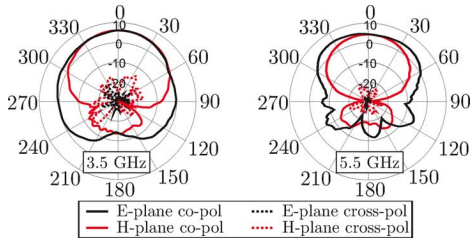

Fig. 6. Measured gain patterns of the dual-mode aperture-fed b-DRA of Fig. 4(a). The broadside gain reaches 5.2 dBi at 3.5 GHz and 4.4 dBi at 5.5 GHz.

Two disadvantages of the probe-fed b-DRA can readily be observed in Fig. 3: the high levels of cross polarization and an asymmetry in the E-plane pattern due to the presence of the coaxial probe. Feeding the b-DRAs through an aperture can solve these issues as described in the following.

III. Aperture-Fed Multiband b-DRAs

The coaxial probe is replaced with an aperture to increase the polarization purity and the pattern symmetry of the b-DRA. In that case, coupling to the radiating element is achieved through a slot etched in the ground plane of an open-ended microstrip line. The ground plane keeps the radiating element separated from the microstrip line, and therefore the effect of spurious radiation from the latter is minimized. To demonstrate the design and operation flexibility provided by the aperture-fed b-DRA, two examples of multistructure aperture-fed b-DRAs with dual-band operation are investigated next. These examples aim at illustrating the geometrical versatility of the bridge-shaped resonator as a building element for more advanced DRA configurations.

The first dual-mode b-DRA is depicted in Fig. 2(a). It consists of a dielectric bridge of permittivity $\varepsilon_{r,b} = 40$ and dimensions $a_1 = 20$ mm, $h_1 = 16$ mm, $w_1 = 8$ mm, $t = 1$ mm, which is fed through an aperture of length $l_{\rm s} = 19$ mm and width $w_{\rm s} = 4$ mm. The microstrip line is a 50-Ω line of width $w_m = 2.4$ mm and stub length $P = 3.6$ mm. Centered underneath the dielectric bridge lies a dielectric slab of dimensions $a_p = 13.5$ mm, $h_p = 13.5$ mm, $w_p = 33$ mm and permittivity $\varepsilon_{r,p} = 10$. The role of the dielectric slab in the DRA operation is double: It helps improving the matching between the aperture feed and the dielectric bridge, and it also serves as a radiating element. Hence, a dual-mode operation is obtained from the combination of the resonances of the high-permittivity bridge-shaped resonator and of the dielectric slab. The design process started from separate designs for the bridge and the rectangular DRA. Subsequently, both structures have been combined, and the resulting geometry has been optimized through simulations using Ansoft HFSS. To validate the good dual-mode operation of this DRA configuration, the prototype shown Fig. 4(a) was fabricated with the given dimensions by gluing three plates of ceramic materials. The realization could be simplified by employing molding techniques, which would also increase the mechanical stability of the device.

Fig. 4(b) illustrates the simulated and measured return loss of the device under investigation. It is observed that the device operates in two bands (defined by $S_{11} < -10$ dB) around the frequencies 3.5 and 5.5 GHz with bandwidth of 9.8% and 16.8%, respectively. These frequencies correspond to the frequencies of excitation of the b-DRA mode and the rectangular dielectric slab mode, respectively. This was verified by varying the width $w_{\rm p}$ of the dielectric slab and observing the effect on the return loss. The results of this numerical study are summarized in Fig. 5, where the return loss of the dual-mode b-DRA is illustrated for values of $w_{\rm p}$ ranging between 9.5 and 13. 5 mm, while the other dimensions of the b-DRA remained the same.

It can be observed in the figure that the variation of the width $w_{\rm p}$ of the dielectric slab has a significant effect on the resonance frequency of the second mode (at the higher frequency). This variation is consistent with the increase of resonance frequency observed in rectangular DRAs when the width is increased (see, e.g., [9, Fig. 2.5]). In contrast, the effect on the resonance frequency of the first resonant mode is much smaller and is only expressed in a degradation of the matching. Hence, it can be concluded that the first resonance corresponds to the b-DRA mode, while the second one to the rectangular DRA mode. The gain patterns of the dual-mode b-DRA of Fig. 4(a) are illustrated in Fig. 6 at the frequencies 3.5 and 5.5 GHz. Broadside and symmetric radiation patterns are obtained at both frequencies, with a cross polarization in both planes remaining below -15 dBi. The shape of the patterns is consistent with the model of a magnetic dipole on a ground plane, with measured broadside gain of 5.2 dBi at 3.5 GHz and 4.4 dBi at 5.5 GHz. Those values point out to the high efficiency of the DRA [11].

To further demonstrate the design versatility provided by the high-permittivity bridge-shaped resonator, the dual-band double b-DRA of Fig. 2(b) is described next. The double-b-DRA geometry consists of two nested dielectric bridges of dimensions $a_1 = 20$ mm, $h_1 = 16$ mm, $w_1 = 8$ mm and $a_2 = 10.5$ mm, $h_2 = 9.2$ mm, $w_2 = 11$ mm, respectively. The design is based

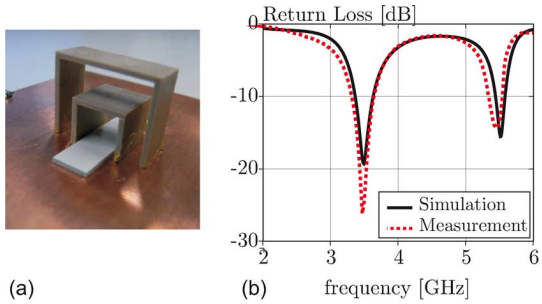

Fig. 7. (a) Fabricated prototype of the double b-DRA. (b) Return loss.

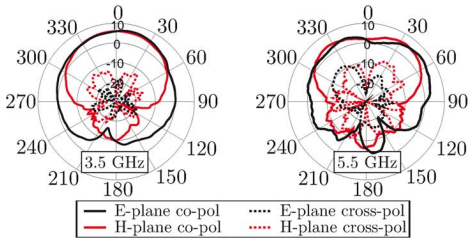

Fig. 8. Measured gain patterns of the dual-mode aperture-fed b-DRA of Fig. 6(a). The broadside gain reaches 4.9 dBi at 3.5 GHz and 0.8 dBi at 5.5 GHz. At 5.5 GHz, the maximal gain in the E-plane is 5.3 dBi.

on two single bridges and has been optimized through simulations to operate at the same frequencies as those in the DRA configuration of Fig. 4(a). The two bridge-shaped resonators have a uniform thickness $t = 1$ mm as well as the same dielectric permittivity $\varepsilon_{r,b} = 40$. The feeding scheme comprises an aperture of length $l_s = 17$ mm and width $w_s = 4$ mm, while the microstrip line has a width $w_m = 2.4$ mm and a stub length $P = 10$ mm. Finally, a nonresonant dielectric slab with dimensions $a_p = 7$ mm, $h_p = 1$ mm, $w_p = 25$ mm and permittivity $\varepsilon_{r,p} = 10$ is used to increase the coupling between the aperture and the two bridge-shaped resonators.

The fabricated prototype of the dual-band double-b-DRA is depicted in Fig. 7(a), while Fig. 7(b) shows the simulated and measured return loss of the device as a function of frequency. It can be observed in the figure that a dual-band operation at the frequencies 3.5 and 5.5 GHz has been obtained with bandwidth of 9.6% and 8.2%, respectively. The agreement between the numerical and the experimental results validates the design concept. To further demonstrate the excellent operation of the double b-DRA at these two frequencies, the measured gain patterns in the E- and H-planes are shown in Fig. 8 in the two operation bands, at the frequencies 3.5 and 5.5 GHz. It is observed that, as expected, the patterns are broadside, while the polarization purity is within acceptable limits (below -12 dB). The measured broadside gain is 4.9 dBi at 3.5 GHz. At 5.5 GHz, the ideally constant E-plane pattern does not result in a broadside maximum because of ripples originating from the finite-size ground plane, but a maximum gain of 5.3 dBi is achieved off broadside.

IV. Conclusion

Several configurations of bridge-shaped DRAs have been introduced in this letter. This type of DRA is an attractive candidate for various applications since it can help overcome several antenna-packaging-related problems and it can be easily designed to exhibit well-behaved multimode operation with broadside patterns and good polarization purity. Two realized representative examples of aperture-fed dual-mode b-DRAs have demonstrated the versatility of these structures.

As a final note, the operational principles of the aperture-fed dual-band b-DRAs can be further extended for multiband operation. For instance, a triple b-DRA or a double b-DRA coupled with a rectangular dielectric slab can be designed to exhibit a reasonably well-behaved triple-band operation. The main limitation of this principle is associated with the increase in the mutual coupling between the radiating elements as their number increases. However, even if such a problem is difficult to be handled analytically, the various numerical techniques that are nowadays available can help optimizing such structures for operation at predetermined frequencies.

Acknowledgment

The authors would like to acknowledge the valuable support from H.-R. Benedickter, M. Lanz, and C. Maccio.

References

[1] S. A. Long, M. W. McAllister, and L. C. Shen, "The resonant cylindrical dielectric cavity antenna," *IEEE Trans. Antennas Propag.*, vol. AP-31, no. 3, pp. 406–412, May 1983.

[2] A. Buerkle and K. Sarabandi, "A wide-band, circularly polarized, magnetodielectric resonator antenna," *IEEE Trans. Antennas Propag.*, vol. 53, no. 11, pp. 3436–3442, Nov. 2005.

[3] G. Almpanis, C. Fumeaux, and R. Vahldieck, "The trapezoidal dielectric resonator antenna," *IEEE Trans. Antennas Propag.*, vol. 56, no. 9, pp. 2810–2816, Sep. 2008.

[4] R. Chair, A. A. Kishk, K. F. Lee, and C. E. Smith, "Wideband flipped staired pyramid dielectric resonator antennas," *Electron. Lett.*, vol. 40, no. 10, pp. 581–582, May 2004.

[5] M. Lapierre, Y. M. M. Antar, A. Ittipiboon, and A. Petosa, "Ultra wideband monopole/dielectric resonator antenna," *IEEE Microw. Wireless Compon. Lett.*, vol. 15, no. 1, pp. 7–9, Jan. 2005.

[6] A. Petosa, N. Simons, R. Siushansian, A. Ittipiboon, and M. Cuhaci, "Design and analysis of multisegment dielectric resonator antennas," *IEEE Trans. Antennas Propag.*, vol. 48, no. 5, pp. 738–742, May 2000.

[7] W. Huang and A. A. Kishk, "Compact wideband multi-layer cylindrical dielectric resonator antennas," *Microw. Antennas Propag.*, vol. 1, no. 5, pp. 998–1005, Oct. 2007.

[8] A. Ittipiboon, A. Petosa, D. Roscoe, and M. Cuhaci, "An investigation of a novel broadband dielectric resonator antenna," in *IEEE Int. Symp. Antennas Propag. Dig.*, Baltimore, MD, 1998, pp. 2038–2041.

[9] K. M. Luk and K. W. Leung, *Dielectric Resonator Antennas*. Hertfordshire, England: Research Studies Press, 2003.

[10] E. H. Lim and K. W. Leung, "Novel application of the hollow dielectric resonator antenna as a packaging cover," *IEEE Trans. Antennas Propag.*, vol. 54, no. 2, pp. 484–487, Feb. 2006.

[11] Q. Lai, G. Almpanis, C. Fumeaux, H. Benedickter, and R. Vahldieck, "Comparison of the radiation efficiency for the dielectric resonator antenna and the microstrip antenna at Ka band," *IEEE Trans. Antennas Propag.*, vol. 56, no. 11, pp. 3589–3592, Nov. 2008.